Determination of Protection System Requirements for DC UAV Electrical Power Networks for Enhanced Capability and Survivability

S. D. A. Fletcher, P. J. Norman, S. J. Galloway, G. M. Burt
Institute for Energy and Environment, University of Strathclyde, UK

Abstract

A growing number of designs of future Unmanned Aerial Vehicle (UAV) applications utilise dc for the primary power distribution method. Such systems typically employ large numbers of power electronic converters as interfaces for novel loads and generators. The characteristic behaviour of these systems under electrical fault conditions, and in particular their natural response, can produce particularly demanding protection requirements. Whilst a number of protection methods for multi-terminal dc networks have been proposed in literature, these are not universally applicable and will not meet the specific protection challenges associated with the aerospace domain. Through extensive analysis, this paper seeks to determine the operating requirements of protection systems for compact dc networks proposed for future UAV applications, with particular emphasis on dealing with the issues of capacitive discharge in these compact networks. The capability of existing multi-terminal dc network protection methods and technologies are then assessed against these criteria in order to determine their suitability for UAV applications. Recommendations for best protection practice are then proposed and key inhibiting research challenges are discussed.

1 Introduction

There has been a recent increase in more-electric aircraft requiring the use of converter fed generation and load systems [1–5]. Whilst this trend is present in all aerospace sectors, it is perhaps most evident in Unmanned Aerial Vehicle (UAV) applications where novel technologies are driving the requirement for greater electrification of secondary systems [6]. New aircraft designs typically employ multiple power electronic converter systems for power conversion and conditioning as well as utilising dc for part or all of the power distribution network in order to capitalise on efficiency, flexibility and power density benefits [3, 5, 7, 8]. However the lightweight and effective

protection of power dense, physically compact dc networks represents a significant barrier to more widespread adoption of dc power distribution for aircraft applications [7, 9, 10].

There has also been a rise in interest in the use of dc power distribution in other applications, including shipboard power systems and microgrids [9, 11–13]. As such, there has been considerable attention in recent years on developing novel protection systems for these applications which seek to overcome the inherent challenges associated with dc [12, 13]. The opportunity now exists to build upon recent research into the protection of multi-terminal dc systems by addressing the protection requirements unique to UAVs and identifying suitable methods to meet these requirements.

This paper will present an analysis of the natural fault response of power electronic fed, compact multi-terminal dc power distribution networks, typical of those proposed for future UAV designs. Key factors such as the peak magnitudes and formation times of fault current profiles are determined and quantified, as a function of network parameters, in order to establish the operating requirements for associated protection systems. Secondary fault effects such as voltage transients are also identified and quantified to illustrate the impact of suboptimal protection system operation. Based on this information, the desired optimal protection approach is identified. The capabilities of different methods and technologies for achieving these aims are then analysed and the most promising of these are identified. Finally, the paper concludes by outlining the protection challenges requiring further attention.

2 Analysis of Compact DC Networks Fault Response

This section will present analytical expressions to describe the typical fault response of compact dc networks. It will initially draw from methods presented in existing literature [14, 15], but will build upon these to reflect the particular characteristics of physically compact dc networks proposed for UAVs.

To analyse the general fault behaviour of a physically compact dc network, consider the example network shown in Fig. 1. This network has been designed by the authors to be representative of a dc UAV network. The network employs Voltage Source Converters (VSC) to interface generators and ac loads to the network, which utilise capacitive only filters as is often the case within multi-terminal dc networks [7, 12, 13, 16–18]. Table 1 presents the network parameters for Fig. 1. These parameters were selected as representative values and derived from a number of sources [19–21].

Considering the response to the busbar fault illustrated in Fig. 1, there are two main sources of fault current. Typically for compact dc networks, the

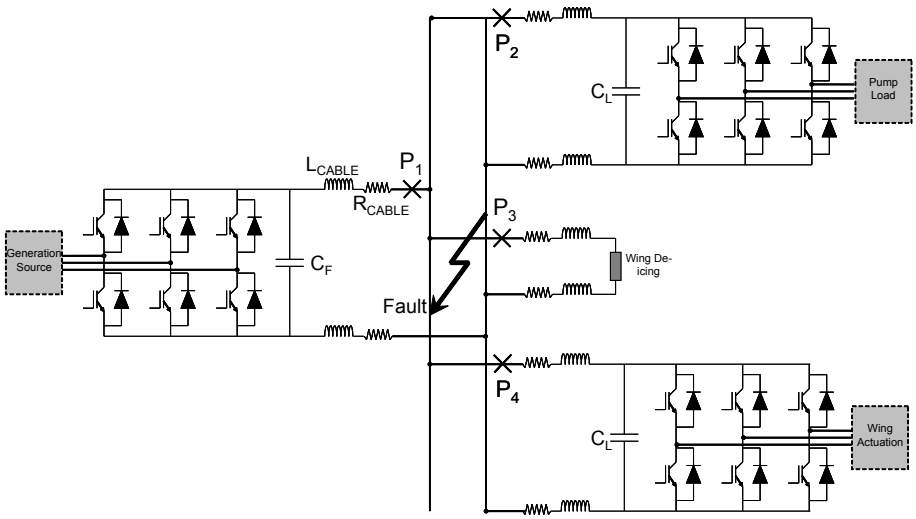

Figure 1: Example multi-terminal dc network

Table 1: Network Parameters

$Voltage$	P_{GEN}	P_{LOAD}	R_{CABLE}	L_{CABLE}	C_F	C_L
270V	20kW	6kW	0.801mΩ/m	0.65μH/m	10mF	0.5mF

discharge of the filter capacitors throughout the network dominates the fault current profile immediately following the fault, whilst the contribution from converter interfaced generation sources and loads (where applicable) forms the latter part of the response [9, 12, 15]. This fault current is illustrated in Fig. 2.

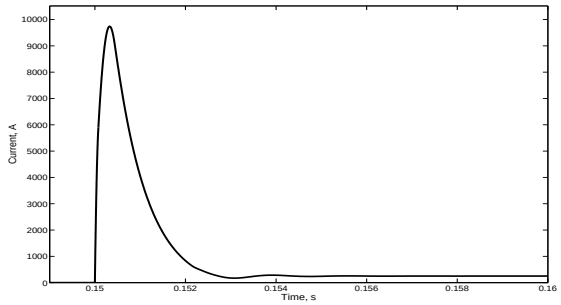

Figure 2: Fault current for a short-circuit fault on the busbar at 0.15s

Fig. 2 illustrates that the potential peak current resulting from the discharge of network capacitors is around 9.74kA without the operation of any protective devices. A fault response of this type can cause two major issues for the protection of the network. First, a current discharge of this magnitude and rate of change has the potential to cause damage to both the capacitors themselves and any sensitive components in the network, such as power electronic switches [12, 22], as well as induce large short term

electromagnetic forces on conductors [23]. Second, the peak of 9.74kA is approximately 130 times greater than the sustained converter contribution. Whilst this response will change with the network impedance characteristics, filter size and configuration and the converter and generation technologies employed, it is clear that such disparity between transient and steady state conditions will cause problems for the protection of the network. These aspects will be addressed in more detail in later sections.

Given the severity and dominance of the initial fault transient, this paper will focus primarily on the natural response of the dc network under fault conditions. This approach will characterise the capacitive discharge in appropriate detail and so aid in determining the electrical protection system requirements for future UAV applications. Note that this focus is in contrast to that taken by other literature on multi-terminal dc network protection, reflecting the unique attributes of the UAV systems being considered in this paper.

2.1 Analysis of Capacitor Discharge

Under short circuit conditions, charged filter capacitors act as high fault level sources. These capacitors, in conjunction with low impedance interconnecting cables (associated with the physically compact nature of the UAV electrical systems), create conditions for rapidly developing and potentially severe short circuit faults, as is illustrated in Fig. 2. This effect is less evident in other applications which utilise longer, higher impedance interconnections.

The typical fault current profile from discharging capacitors can be described by considering the natural response of an equivalent RLC circuit (as illustrated in Fig. 3) with appropriate initial capacitor voltage and inductor current representing pre-fault network operation. Equivalent second order circuits and expressions are used throughout the analysis in order to best illustrate behaviour and derive the parameters of interest. Expansion of the analysis to cover multiple RLC branches can result in much larger analytical expressions with which it becomes far more difficult to derive useful parameters. For these higher order expressions, early substitution of parameter values is recommended [24].

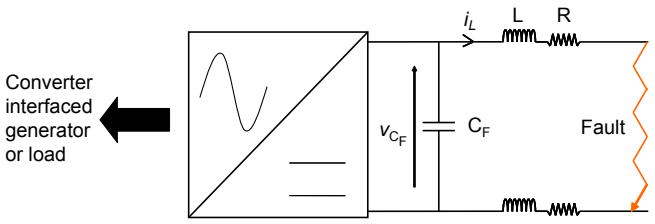

Figure 3: Equivalent circuit for the faulted network

The natural response of the RLC circuit illustrated in Fig. 3 can be defined in two separate phases [17]. These are covered in the following two subsections.

2.1.1 First Phase Characterisation

In the Laplace domain, the RLC circuit response is

$$i(s) = \frac{\frac{v_{CF}(0)}{L} + i_L(0)s}{s^2 + \frac{R}{L}s + \frac{1}{LC_F}} \tag{1}$$

where $i_L(0)$ is the initial current through the inductor and $v_{CF}(0)$ is the initial voltage across the capacitor C_F. The resistance R represents the combined sum of the line resistance of both cable connections to the converter plus equivalent series resistance of the filter capacitor. Similarly, the inductance L represents the total line inductance of both incoming and outgoing cables (the capacitor equivalent series inductance is usually insignificant compared to this). The expression in (1) assumes that any changes in the output of the converter are negligible in comparison to the magnitude of the discharge current for the period immediately following the occurrence of the fault [15].

Taking the inverse Laplace transform of (1), the general current representation in the time domain is

$$i(t) = A_1 e^{s_1 t} + A_2 e^{s_2 t} \tag{2}$$

where $A_{1,2}$ are coefficients which depend on initial conditions and $s_{1,2}$ are the roots of the characteristic equation (the denominator of the Laplace expression) which are equal to

$$s_{1,2} = -\alpha \pm \sqrt{\alpha^2 - {\omega_0}^2}. \tag{3}$$

In (3), α is the damping factor (or Neper frequency) and is defined as

$$\alpha = \frac{R}{2L}. \tag{4}$$

The term ω_0 is the resonant radian frequency and is defined as

$$\omega_0 = \frac{1}{\sqrt{LC_F}}. \tag{5}$$

In (3), the relative magnitudes of α^2 and ω_0^2 determine the form of the current response, where $\alpha^2 > \omega_0^2$, $\alpha^2 = \omega_0^2$ and $\alpha^2 < \omega_0^2$ represent over, critically and underdamped fault responses respectively. For underdamped systems, the roots $s_{1,2}$ are complex and the current response is oscillatory. Applying the Euler identity to (2) and substituting terms for initial conditions, the underdamped current response can be derived as

$$i(t) = \frac{v_{CF}(0)}{L\omega_d} e^{-\alpha t} \sin(\omega_d t) + i_L(0) e^{-\alpha t} \left[\cos(\omega_d t) - \frac{\alpha}{\omega_d} \sin(\omega_d t) \right]. \quad (6)$$

In (6), ω_d is the damped resonant frequency and is defined as

$$\omega_d = \sqrt{{\omega_0}^2 - \alpha^2}. \quad (7)$$

As a result of the large filter capacitance and relatively low cable inductance (resulting from the short cable lengths associated with UAV network applications), the dominant part of any underdamped fault current characteristic shown in (6) is due to the initial voltage across the converter filter capacitance. As such, the expression for fault current profile can be reduced to

$$i(t) \approx \frac{v_{CF}(0)}{L\omega_d} e^{-\alpha t} \sin(\omega_d t). \quad (8)$$

For highly underdamped conditions (where $\omega_0^2 >> \alpha^2$ and ω_d tends to ω_0) (8) can be further reduced to

$$i(t) \approx \frac{v_{CF}(0)}{Z_0} e^{-\alpha t} \sin(\omega_0 t), \quad (9)$$

where Z_0 is the surge impedance of the fault path and is defined as

$$Z_0 = \sqrt{\frac{L}{C_F}}. \quad (10)$$

The time taken for the current magnitude to reach its peak magnitude can be derived from (8) by equating its derivative to zero and solving for t. This derivation is results in

$$t_{peak} = \frac{1}{\omega_d} \arctan \frac{\omega_d}{\alpha}. \quad (11)$$

Again, for the underdamped case where $\omega_0^2 >> \alpha^2$, and ω_d tends to ω_0, (11) reduces to

$$t_{peak} \approx \frac{1}{\omega_0} \arctan \frac{\omega_0}{\alpha}. \quad (12)$$

Using a similar approach, expressions for peak fault current magnitude and time to peak for overdamped networks (where the roots $s_{1,2}$ are real) can be developed. The current and peak time equations are

$$i(t) = \frac{v_{CF}(0)}{L(s_1 - s_2)} \left(e^{s_1 t} - e^{s_2 t} \right) \quad (13)$$

and

$$t_{peak} = \frac{\ln\left({}^{s_2}/_{s_1}\right)}{s_1 - s_2} \tag{14}$$

respectively. Equations (13) and (14) can also be applied to find the underdamped response. However the complex roots $s_{1,2}$ make these expressions difficult to solve manually.

The unlikelihood of a critically damped fault response occurring is such that derivation of specific equivalent expressions within this paper would be of little benefit.

2.1.2 Second Phase Characterisation

In compact dc electrical networks the time to peak for the capacitor discharge current is typically very short [12], and as such it is also important to consider the second phase of the fault current profile which usually occurs shortly after the current peak. It is worth noting that this aspect is not typically considered for most multi-terminal dc network applications [9] as there is a much longer time peak within which the protection systems are expected to operate. However, this is not necessarily a valid assumption for compact systems.

The analysis of the second phase of the fault current profile is notably different to that associated with the characterisation of the first phase. This is a result of the presence of freewheeling diodes in parallel with the active devices within the VSC [12, 16, 17].

Following the occurrence of the peak current, L-C oscillations in the circuit can cause the voltage across the converter's filter capacitor to become negative [17]. This has the effect of reversing the voltage at the converter terminals and, provided this voltage is sufficiently high, causing the freewheeling diodes to conduct. This provides an alternative current path, regardless of the state of the active switching devices within the converter, and so changes the response of the network. Fig. 4 shows an equivalent circuit which can be used to represent the generation and active load interface in the network shown in Fig. 3 during the period of voltage reversal. In this figure, V_d is equal to the sum of the diodes' on-state voltages in any converter leg and R_d is equal to the series and parallel combinations of the diodes' on-state resistances.

In a similar manner to that previously presented, expressions defining the behaviour of the reverse polarity circulating current can be derived. The general expression for current $i(t)$ is

$$i(t) = \frac{v_d}{R_d + R} + A_1 e^{s_1 t} + A_2 e^{s_2 t}, \tag{15}$$

where the roots $s_{1,2}$ are defined in (3) and

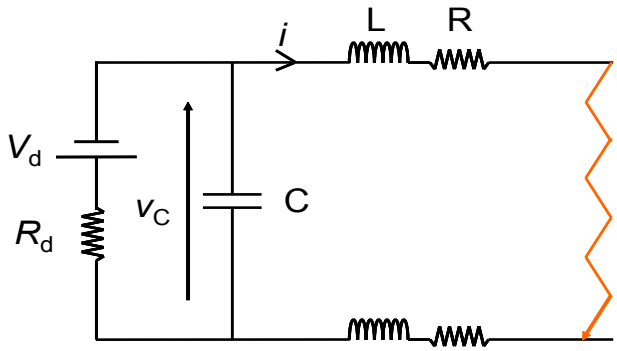

Figure 4: Equivalent circuit of the faulted circuit with conducting freewheeling diodes

$$\alpha = \frac{R}{2L} + \frac{1}{2R_d C}, \tag{16}$$

$$\omega_0 = \frac{1}{\sqrt{LC}} + \frac{R}{\sqrt{R_d LC}}, \tag{17}$$

$$A_1 = i(0)(s_2 + \frac{R}{L}) - \frac{v_C(0)}{L} - \frac{v_d s_2}{R_d + R}, \tag{18}$$

$$A_2 = i(0) - A_1 - \frac{v_d}{R_d + R}. \tag{19}$$

Equations specific to damping conditions can be found using methods from the previous section.

To assess the period of this second phase of the fault response, the voltage across the diode-capacitor parallel branch must be derived (as this indicates when the reverse voltage is greater than the turn on voltage of the diodes). The diode-capacitor parallel branch voltage is equal to the voltage across the line resistance R and inductance L, assuming the voltage developed across the fault is negligible. Therefore, the voltage $v(t)$ across the diode-capacitor parallel branch is

$$v(t) = i(t)R + L\frac{di}{dt}. \tag{20}$$

By employing methods already demonstrated and substituting using the expression for current $i(t)$ given in (15), this expression can be expanded to give

$$v(t) = \frac{v_d}{R_d + R} + (R + s_1 L)A_1 e^{s_1 t} + (R + s_2 L)A_2 e^{s_2 t}. \tag{21}$$

Equation (21) is transcendental, therefore iterative numerical methods are required to find the duration of the freewheeling diode conduction. One such numerical method is Newton's Method, which can be expressed as

$$t_{n+1} = t_n - \frac{V(t_n)}{V'(t_n)} \tag{22}$$

where t_n is the time at which (21) is evaluated and $V(t_n)$ and $V'(t_n)$ are the voltage and derivative voltage respectively at t_n.

To solve for the period of diode conduction, $v(t)$ in (21) should be set equal to the combined switch-on voltage of the diodes in the conduction path within the converter. It is likely that two solutions exist to (22), the first as the diode begins to conduct (at $t = 0$) and the second as the diode ceases conduction. To aid the convergence of (22) towards the latter, t_n should be given a non-zero initial value.

After the time in (22) elapses, the circuit returns to its previous operating characteristic, albeit at a lower current magnitude due to the energy dissipated within the diodes.

2.2 Illustration of Unique UAV Network Attributes

The characteristics of compact dc UAV networks are such that under short circuit fault conditions, current response is likely to be underdamped (this is illustrated in the following case study). In contrast, many other multi-terminal dc networks considered within the literature represent overdamped cases due to their longer line lengths (and hence reduced resonant frequencies). The differences between these can have significant implications for the operating requirements of associated protection systems.

To illustrate this aspect, table 2 shows the parameters of a typical UAV network (as shown in Fig. 1) compared to that of a dc microgrid [13]. The peak magnitude and time to peak for the fault currents associated with the generator interfaces of these networks are also presented and are calculated using the expressions derived earlier for underdamped (UAV network) and overdamped (microgrid) responses.

It can be seen from these results that the peak current in the typical UAV network is of similar magnitude; however, importantly, it occurs far earlier than in the microgrid network. While both fault transients are large in magnitude (for low voltage distribution systems), the rapid fault development in the UAV network in particular creates far more demanding operating requirements for the network protection system, an aspect which is explored further in later sections.

The key factors in the difference in fault response characteristics demonstrated in table 2 are as a result of the difference in voltage levels, cable inductance and resistance per unit length and size of the rectifier filter capacitor. Whilst this reflects the impact of the chosen application and as-

Table 2: Network Parameters

Parameters/Network Type	UAV	Microgrid
Operating Voltage (V)	270	400
Main filter capacitance size (mF)	10	56
Capacitor equivalent series resistance (mΩ)	5	2
Cable inductance (μH/m)	0.65	0.34
Cable resistance (mΩ)/m)	0.801	0.641
Total cable length in fault path (m)	10	60
Time to fault current peak (μs)	357.0	1048
Peak magnitude of fault current (kA)	7.49	7.41

sociated technologies on fault response, it does mask the impact of cable length (and associated network damping levels), which is also a key distinguishing feature of electrical networks for UAVs compared to those for other applications.

As such, a second comparison will also be shown in which the network voltage and main filter capacitance of the UAV network are made equal to that of the microgrid. This gives values for time to peak and peak current magnitude of 741.0μs and 20.98kA respectively. As with the previous comparison, the modified UAV network fault current peak occurs prior to that of the microgrid system but is now also much larger due to a reduction in surge impedance. This example serves to illustrate how line length has a large bearing on the response of the network, and why the protection challenges for compact networks, such as those on UAVs, are more significant.

2.3 Contribution from Converter Interfaced Sources

Whilst this paper emphasises the role of the natural response of the aircraft network in determining the protection system operating requirements, it is essential not to overlook the contribution from other sources, such as that of converter interfaced sources [16, 17, 25] and energy storage systems [13, 15, 26] (depending on the technologies and control strategies employed). Indeed, substantial research has been conducted on the behaviour of these systems under fault conditions, which is largely applicable to UAV applications [13, 17, 25, 26]. Perhaps the key areas of interest are the impact of novel generation types not typically seen in other multi-terminal dc network applications, such as switched reluctance and permanent magnet synchronous machines [7]. In particular, the specification of an integrated protection system that inherently accommodates the natural characteristics of these technologies would be of great value. However, this aspect is outwith the scope of this paper.

2.4 Consideration of Converters Containing Series Inductive Filters

Whilst the majority of proposed network architectures for future dc networks, which employ VSCs, operate without the use of inductive filters [7, 12, 13, 16–18], the potential impact of these devices on the fault response makes them worthy of consideration. Assessment of the impact of inductive filters can be easily accommodated into the analysis presented earlier in this section by setting inductance L equal to the sum of line and filter inductances. The additional inductance decreases the damping in the network, hence the example UAV network would remain underdamped, so equations (8) to (12) still apply to this analysis.

The impact of the inductive filter on the peak fault current can be assessed using (9). If it is approximated that the peak current is equal to $\frac{v_{CF}(0)}{Z_0}$ then the peak becomes proportional to $\sqrt{L}$, i.e. increasing L by 50 times, decreases the current peak by 7.07 times. As resistance is not included in this calculation, the impact of inductance is at its maximum and hence $\sqrt{L}$ is the maximum by which the current peak changes. Relating this to table 2, including resistance parameters, an increase of L by 50 times results in a peak current from C_F of 2309A, which equates to a decrease of 3.24 times the figure reported in table 2. Whilst there is a substantial decrease in fault current, the disparity between peak transient and steady state fault currents still exists and hence the problems for fault detection remain.

Of perhaps more significance is the impact of the additional inductance on the rise time and time to peak of the current response. This can be assessed using (11), from which it can be calculated that with 50 times greater L, $t_{peak} = 2.8ms$, representing close to an order of magnitude time difference in reaching the current peak compared to table 2. Depending on the protection operating strategy, this potentially allows more time for the detection and isolation of faults, reducing demands on the protection system.

The reduction in fault current and increase in rise time suggests that, in terms of fault response, an additional series inductance can be beneficial. However, as later sections of this paper discuss, their inclusion can increase system size and weight and contribute to undesired post-fault clearance transients. Furthermore, addition network inductance can increase circuit breaker voltage and energy dissipation requirements and fault clearance time, however the assessment of this is outwith the scope of this paper. Therefore the remainder of this paper focuses on a more optimal solution, without the use of inductive filters, based on extremely fast acting protection.

3 UAV Electrical System Protection Challenges

It is important to review how the unique attributes of UAV networks introduced in section 2 and the general requirements of aircraft electrical power systems, such as greater safety criticality [6], impact on the UAV protection system requirements. The key challenges associated with the protection of UAV electrical networks can be broadly categorised under three main headings. These are discussed in the following subsections below.

3.1 Fault Severity

Section 2 illustrates how the presence of high fault level sources, such as filter capacitors, within physically compact networks can lead to the creation of electrical faults which are both rapidly developing and severe in nature. Despite the relatively small amount of energy in terms of Joules (determined by $\frac{1}{2}CV^2$) in the capacitors, the substantial current magnitude and high rate of discharge has the potential to cause damage to both the capacitors themselves and any sensitive components in the network such as power electronic switches [12, 22]. There is however substantial i^2t fault energy in this initial fault transient relative to the converter input. For example consider the fault current plot in Fig. 2. The i^2t over the transient period is $56.2kA^2s$ (at 3ms after the fault). For a constant steady state fault current input of 74.07A (20 kW at 270V) it would take approximately 10.2s to reach the same i^2t value.

For safe operation, the electrical network and associated protection system must be capable of responding to such conditions in order to limit any potential damage caused by an electrical fault, maximising the survivability of the UAV.

3.2 Safety Criticality

In future UAV applications, there is likely to be a greater reliance on electrical systems for safe flight [6]. This makes the implications of electrical faults or failure more significant than in other non-aviation applications, where short outages may be tolerated [13, 16]. This safety critical aspect leads to a requirement for the protection system to provide higher levels of selectivity than necessary in other applications in order to maintain electrical supply to critical loads.

3.3 Weight Criticality

In order to capitalise on efficiency benefits associated with increased electrification, the total electrical system weight (including protection system components) must be minimised [1]. This requirement can restrict both the size and rating of the electrical loads and converters and the amount

of protection equipment that can be placed on the network. This aspect is typically in direct opposition to the requirement for a very safe, redundant and reconfigurable network design and protection system.

4 Maximising UAV Survivability

Taking the protection system requirements from section 3 into account, this section investigates the options for how they may be achieved. To ensure safe operation of any electrical network during fault related transients there are four general approaches:

1. Design the network components to withstand and ride through the transient conditions.

2. Place suppression devices (such as snubbers) in the network to reduce the severity of the transients to acceptable levels.

3. Provide redundancy in the network functionality such that if any component or group of components is adversely affected by a fault transient, a backup healthy system is available.

4. Install a fast acting protection system to isolate the fault before the severe transient develops.

In practice, it is likely that a suitable mix of all four methods would be applied within a network design. However, the extent to which each is employed is dependent on the requirements of the application. For future UAV applications, the first three methods could represent a substantial increase in overall system size and weight and as such are less desirable than the fourth option. Indeed measures 1-3 would be utilised more extensively if the protection system could not be designed to operate quickly enough to limit the extent of the fault related transient. In current aircraft designs, the safety critical nature of the electrical system is such that option 3 is often extensively employed [27].

The fourth option presents what appears to be the ideal, and novel, solution and this is the focus of the research reported in this paper. It is a potentially lightweight method (as it does not require any additional components unlike options 1-3 above) and would minimise both damage to components and disruption to the rest of the network due to the early interruption of the fault. This however is a very challenging solution to implement. In order to isolate the fault before the severe transient fully develops, the authors propose that the protection system should operate before the current peak. However, section 2 has shown that the time to peak for UAV networks can be far less than a millisecond. Comparing this time with the standard response and protection operating time of aircraft

systems [28–30], it can be seen that the associated protection system requires a much faster response than is currently implemented.

5 Impact of Protection System Operating Time on Local Voltage Transients

In addition to the reasons given in the previous section, there are other drivers in moving towards the application of fast acting protection systems for UAV applications. Namely, the effect of breaker operation on induced voltage transients within the network.

5.1 Converter Voltage Reversal

Section 2 discusses a situation where, following the occurrence of the fault current peak, the voltage at the converter terminals can reverse, causing current to flow through the freewheeling diodes of the converter. This section presents expressions to quantify the magnitude of this reverse polarity current and discusses the protection issues that may arise from this behaviour.

The total current through all of the converter's freewheeling diodes can be expressed as a function of the voltage $v(t)$ in (21) and diode parameters V_d and R_d. Equation (22) provides the time period of this current conduction. Current through the freewheeling diode path $i(t)$ is therefore

$$i(t) = \frac{v(t) - V_d}{R_d}. \tag{23}$$

The effective total on-state resistance of the freewheeling diodes (R_d) is typically in the order of a few milliohms [31] and as such, even small voltage reversals may result in significant currents flowing through these diodes. This presents a risk of the diodes being damaged and the active switch overcurrent thresholds being exceeded, causing the converter to shut down (if it has not done so already).

In order to accommodate this risk, potential solutions include using diodes with higher rated transient current withstand or installing current suppression devices to reduce the initial transient. Either option is likely to have associated space and weight penalties. These options can be avoided if the relevant protection systems can be guaranteed to operate before the voltage reversal occurs.

5.2 Overvoltage Transients

Section 3 discussed the benefits of utilising fast acting protection within UAV applications. However, consideration must also be given to the transient voltage effects produced by operating at near peak fault current levels.

Previous research by the authors has shown how the redistribution of significant amounts of stored inductive energy created during fault conditions can lead to significant post-fault voltage transients propagating throughout the remaining healthy portions of the network, due to the operation of network protection [32, 33].

To illustrate this effect, consider a scenario where a fault has occurred at a load and the fault is subsequently cleared, disconnecting the load from the network. The response of the remaining network will be analysed using a simplified equivalent circuit shown in Fig. 5 which consists of the filter capacitance at the converter output C_1, line resistance R and inductance L, and the total capacitance of the remaining load converters C_2.

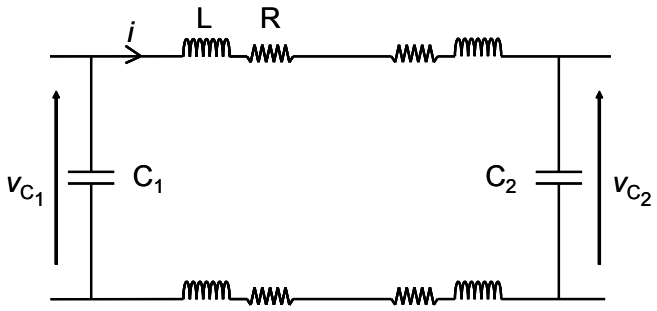

Figure 5: Equivalent circuit for the post fault clearance network

The resultant circuit in Fig. 5 consists of the filter and load capacitors in series with the line resistance and inductance. This circuit configuration permits the second order analysis described in section 2 to be applied. Assuming the response is underdamped, the current flowing in the line following the clearance of the fault is

$$i(t) = \frac{v_{C1}(0) - v_{C2}(0)}{L\omega_d} e^{-\alpha t} \sin(\omega_d t) + i(0) e^{-\alpha t} [\cos(\omega_d t) - \frac{\alpha}{\omega_d} \sin(\omega_d t)] \quad (24)$$

where all initial conditions reflect the currents and voltages at all the circuit locations at the time of protection operation. The total capacitance C is now equal to the series combination of the load and filter capacitors, which varies C in (5), changing ω_0 (and hence ω_d) in the post-fault network. The subsequent voltage response across the load capacitance will be

$$v(t) = \frac{v_{C1}(0)C_1 + v_{C2}(0)C_2}{C_1 + C_2} + \frac{(v_{C1}(0) - v_{C2}(0))C_1 e^{-\alpha t}}{C_1 + C_2} \times \left[-\cos(\omega_d t) - \frac{\alpha}{\omega_d} \sin(\omega_d t) \right] + \frac{i(0) e^{-\alpha t}}{C_2 \omega_d} \sin(\omega_d t). \quad (25)$$

In (25) the first two terms show the charging effects of the larger filter capacitance C_1 on the smaller load capacitance C_2, similar to that of the transient recovery voltage [24] common on power systems. For highly underdamped networks, v_{C2} can reach approximately twice the magnitude of $V_1(0)$, provided $C_1 >> C_2$. However, previous studies by the authors [32,33] have shown that while the voltage difference does have an impact on the transient voltage, if high currents are being interrupted, the dominant term in (25) is likely to be that of the initial current (I_0). Taking this into account, (25) shows that the higher the breaking current and the smaller the remaining load capacitance, the greater the magnitude of the subsequent voltage transient.

To illustrate how the maximum voltage transient changes with time, the network in Fig. 1 was simulated with a fault across the pump load. The nearby circuit breakers were then set to operate for a range of fault clearance times after fault inception. The results are illustrated in Fig. 6, where maximum transient voltage magnitude is plotted against circuit breaker operating time and fault current at the time of protection operation. The voltage difference between the load and filter capacitors is also shown in the subplot to illustrate its effect on maximum transient voltage magnitude.

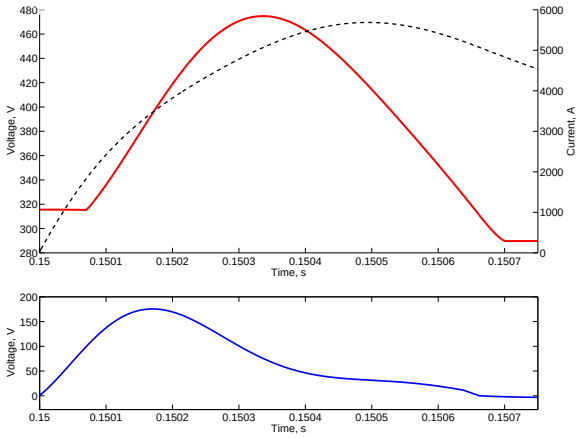

Figure 6: Maximum voltage transient caused by circuit breaker operation (upper plot - solid line) after a short circuit fault occurs at 0.15s compared to varying initial conditions. Potential fault current (upper plot - dashed line), capacitor voltage difference (lower plot).

Fig. 6 illustrates that there is a period after the fault inception where the operation of protection may cause voltage spikes of up to 1.75 times the nominal system voltage at load converter terminals. The peak voltage transient is shown to occur just before the interruption of peak fault current. It does not coincide exactly with the peak current due to the changing voltage difference between the load and filter capacitors.

Given that the capacitors considered in this example are connected across converters, care must be taken that these converters are not damaged through fault clearance events [34], or almost as importantly, do not trip due to overvoltage protection operation. Either of these events could results in the effects of the fault propagating into healthy parts of the network causing cascaded tripping and equipment damage.

As in previous sections, solutions to the issue of overvoltage transients include up-rating components [34], employing voltage suppression devices, both of which have associated weight penalties, or operating the circuit breakers early enough in advance of the fault current peak. The latter option is consistent with previously discussed requirements for voltage reversal prevention and maximisation of vehicle survivability and is hence the preferred, although most demanding, solution.

6 Determination of Protection System Operating Requirements

Within sections 4 and 5 it was concluded that the presence of a fast operating and selective protection system could minimise the overall weight of a future UAV electrical system whilst providing key benefits in survivability and minimisation of fault effects. This section will utilise the analysis conducted in section 2 to determine the key operating requirements for the UAV electrical protection systems such that these benefits may be realised.

The total protection operating time can be generally defined in two discrete stages; first, the time to detect and locate the fault and determine the appropriate course of action and second, the time for the breaker to operate. The former is a function of the detection method, and the latter relates to the capabilities of dc circuit breaker technologies. The following subsections will consider these aspects in more detail, starting with the circuit breaker technologies.

6.1 Implications for Circuit Breaker Technologies

In order to better appreciate the applicability of different circuit breaker types to the proposed fast acting UAV electrical network protection system it is first necessary to consider the range of typical operating times. Fig. 7 shows operating times of solid state (SSCB) [22, 35], hybrid (HCB) [36, 37] and electro-mechanical circuit breakers (EMCB) [38, 39] in relation to a typical time to peak for fault currents within UAV and microgrid electrical networks (based on the values derived in section 2). Whilst the actual time taken for the fault current to reach its peak may vary, this specific example provides a good illustration of the impact upon the choice of circuit breaker technologies for the two applications.

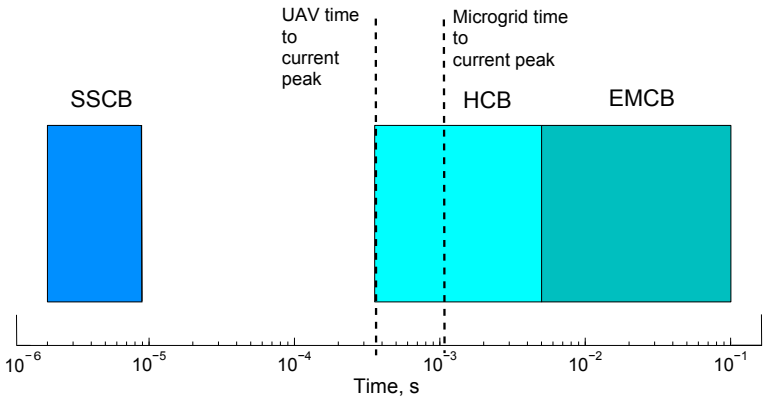

Figure 7: Comparison of circuit breaker operating times

Fig. 7 shows that the typical operating times of EMCBs are far greater than that required for UAV applications. The quickest operating HCBs may be suitable for this application although options for their use would be limited as there would be little additional time for fault detection and location. Interestingly, HCBs may, however, be the technology of choice for microgrids where a longer time to peak is anticipated.

The comparison between circuit breaker operating times and typical times to peak suggests that only SSCBs are truly suited for use within UAV networks. These also represent the most lightweight solution. Whilst few, if any, commercially available devices exist for the voltage levels proposed for future UAV applications which have high enough current break capabilities for the currents described in section 2 [40], the development of these technologies will provide greater opportunity for use in future systems. Certainly, without the availability of these technologies, truly optimised protection of dc UAV networks will be very challenging.

6.2 Implications for Fault Detection and Location Methods

Fig. 7 also provides a basis for determining the maximum permissible fault location times of the aircraft protection system. This is simply,

$$t_{Location} < t_{peak} - t_{CBoperation} \tag{26}$$

where $t_{Location}$ is the required time for the protection system to send a trip signal to the associated circuit breakers (from the time of fault inception) in order to ensure circuit breaker operation prior to the occurrence of the fault current peak.

Fig. 7 and table 2 indicate that, acting in conjunction with SSCBs, any protection system must locate the fault within approximately 300μs in order to operate the circuit breaker before the current peak (or perhaps even less depending on the network specific requirements for avoiding the creation of

post-fault overvoltage transients).

The achievement of this is constrained by the bandwidth of sensing technologies and grading methods used to ensure coordination between multiple protection devices. Therefore the performance of various protection schemes, when operating within such time constraints, is an area of great research interest. The following section assesses the options for matching this strict operating criterion.

7 Evaluation of Protection Method Suitability for Future UAV Applications

This section will briefly review the capability of both established and novel protection techniques to achieve the functional requirements laid out in the previous section. It will also highlight where these protection systems must be developed and refined in order to be suitable for UAV applications.

7.1 Non-unit Protection Implementation Challenges

Non-unit protection does not protect a clearly bounded zone of the power system and will operate whenever its threshold is violated; non-unit schemes have inherent backup capabilities and will act to protect the system if a neighbouring protection system fails to operate [41].

Due to the high fault levels under short circuit fault conditions, non-unit techniques, and in particular overcurrent, can be utilised to very rapidly detect faults. For example, the authors in [12] propose the use of instantaneous overcurrent protection inherent in power electronic switches to interrupt capacitive discharge currents far faster than the 300μs protection operation targets set out in section 6. However when higher levels of selectivity, i.e. ensuring that only the local protection operates for a fault at a particular location in the network, are desired, issues can arise in the implementation of overcurrent protection, especially where instantaneous overcurrent protection is utilised. This is the case even where multiple relays are graded using overcurrent protection in highly capacitive networks. For example, if molded-case circuit breakers (MCCB) are utilised at P_1 and P_2 in Fig. 1, for a fault across the pump load, the initial discharge current can be high enough to occupy the instantaneous trip region of both MCCBs [42], potentially tripping both P_1 and P_2 or even just P_1 [9]. This would cause significant protection coordination issues and unnecessary isolation of non-faulted elements of the system, which would potentially have grave consequences in an aerospace application. In addition, implementing overcurrent grading based on sustained overcurrent levels would not give the desired result for protection operation within the transient region.

For non-unit methods there is also the issue of variable fault resistance

and the impact this has on fault current. Section 2 provides analysis to determine currents with various damping conditions and from (6) and (13), it can be found that as the total resistance of the fault current path increases, the capacitive fault current greatly decreases. This is a particular issue for compact networks where, due to small line impedance, any fault resistance will make up a greater proportion of overall fault path impedance. Also, the fault resistance is variable, which can lead to similar responses being presented for many different fault locations, leading to protection selectivity issues.

As a result of these selectivity issues, the authors believe that methods such as the instantaneous overcurrent trip on capacitor output presented in [12], which do meet the operational time requirements, are unsuitable where highly selective network protection is desirable. For example, instantaneous overcurrent protection, located at the filter capacitor output in Fig. 1, could potentially lead to the isolation of this capacitor for load faults, e.g. a fault on the wing de-icing system, due to the high initial fault current. This would lead to the uncoordinated tripping of this capacitor's breaker (when downstream protection should isolate the fault) and delayed or non-tripping of load protection due to the removal of the main fault current source. Furthermore, power quality may be degraded for the period of capacitor disconnection. As previously stated, unnecessary removal of non-faulted elements of the electrical system has potentially disastrous consequences in aircraft.

Similarly, rate of current change methods for monitoring capacitor output [13] are sensitive to fault resistance in compact systems, and so similar issues exist for fault selectivity for networks utilising such protection methods.

7.2 Unit Protection Implementation Challenges

Unit protection protects a clearly bounded zone of the power system and will not operate for faults external to this zone. In contrast to non-unit schemes, it does not provide backup to adjacent elements of the system [43].

Current differential protection operates by comparing all currents' magnitudes and/or relative directions at the boundaries of a specified element within a network [43]. The nature of the differential protection method is such that it is far less susceptible to the effects of variable fault levels and impedances than non-unit methods [18, 44], facilitating effective protection selectivity in the network. However the major challenge is the implementation of a differential protection scheme which allows a trip decision to be achieved within the desired time frame.

Modern differential current schemes propose the use of communications even for relatively compact systems to take advantage of the benefits of IEC 61850 [45], a communication standard for protection and control systems.

However given the inherent processing and communication propagation delays, meeting the stringent time criterion may be challenging when utilising communication networks for this purpose [43]. Furthermore, due to the high rate of change of measured data (average of 21A/μs from fault inception until t_{peak} in table 2 for example) near exact time synchronisation would be required for accurate trip decisions for both high (transient) and low (sustained) fault current conditions. Measurement accuracy may also be an issue for current differential schemes that compensate for current flow to and from the capacitance [46] in the differential calculation. This compensation needs to be performed with high accuracy due to the dominant magnitude of the capacitor fault current. These aspects all provide further challenges for implementation.

7.3 Backup Protection

There remains a requirement to provide backup protection to prevent catastrophic failure in the event of primary protection system maloperation. Backup could be provided by a number of slower acting non-unit methods; a requirement being for these methods to not operate during the initial capacitive discharge to avoid coordination issues with the primary protection system. For example, undervoltage protection could potentially be utilised for this purpose [13]. The presence of a fault will lead to a decrease in dc voltage but this decrease is proportional to the rate of capacitive discharge. If the primary protection is set to operate within the time constraints proposed in section 6 then it will operate prior to the undervoltage protection, provided the voltage threshold is not set too high, and coordination between primary and backup protection systems will be retained.

7.4 Proposed Method of Unit Protection Implementation

Due to the compact size of the UAV network, it lends itself to a pilot wire type scheme [43], where current measurements are directly compared.

To achieve coordinated protection system operation within the derived time constraints using a current differential scheme, the authors propose that the use of a central processing device, comparing current measurements, could be used. This could involve either physically summing currents prior to the central device or the direct input of analogue measurements to the central device, where analogue to digital conversion would take place, before the sum of currents is compared to trip threshold and decision sent to the circuit breakers. Analysis of example processing devices [47, 48] suggests that, even if multiple measurements are compared, the total conversion and processing time is far less than the expected operating requirement. Therefore this approach may be a viable method of implementation for high speed, coordinated protection system operation.

However further research is required to determine whether this type of dc current differential scheme could operate quickly enough to meet the detection requirements and this is an area of continuing interest.

8 Conclusion

This paper has highlighted the specific protection challenges caused by the natural response of highly capacitive dc UAV networks. Analysis is provided to allow these challenges to be quantified in terms of peak current magnitudes and the time to peak from fault inception. From the understanding of network fault response provided by this analysis, the paper has derived an optimal protection strategy, which is proposed as the operation of protection prior to the capacitor discharge current peak. Recognising this optimal protection strategy, the paper has identified potential circuit breaker technologies and quantified the required fault detection times. Finally, the paper has identified the need for further research by highlighting the challenges in achieving the desired protection system performance using both conventional and novel protection methods.

Acknowledgment

The authors are grateful for the support of Rolls-Royce plc through their University Technology Centre programme. The work described in this paper is also supported by the Engineering and Physical Sciences Research Council.

References

[1] J. Rosero, J. Ortega, E. Aldabas, and L. Romeral, "Moving towards a more electric aircraft," *Aerospace and Electronic Systems Magazine, IEEE*, vol. 22, no. 3, pp. 3 –9, March 2007.

[2] K. Emadi and M. Ehsani, "Aircraft power systems: technology, state of the art, and future trends," *Aerospace and Electronic Systems Magazine, IEEE*, vol. 15, no. 1, pp. 28 –32, Jan 2000.

[3] M. Sinnet, "787 No-Bleed systems: saving fuel and enhancing operational efficiencies," in *Boeing Commercial Aeromagazine*, Quarter 4, 2007, pp. 6 – 11.

[4] P. Butterworth-Hayes, "All-electric aircraft research speeds up," in *Aerospace America*, January 2009, pp. 1–7.

[5] J. Bennett, B. Mecrow, D. Atkinson, C. Maxwell, and M.Benarous, "A fault tolerant electric drive for an aircraft nose wheel steering actuator,"

in *Power Electronics, Machines and Drives, 2010. 5th IET Conference on*, April 2010.

[6] N. R. C. Committee on Autonomous Vehicles in Support of Naval Operations, *Autonomous Vehicles in Support of Naval Operations*. National Academies Press, 2005, ch. 3, ISBN: 0-309-55115-3.

[7] S. A. Long and D. R. Trainer, "Ultra-compact intelligent electrical networks," in *1st SEAS DTC Technical Conference*, 2006.

[8] E. Gietl, E. Gholdston, F. Cohen, B. Manners, and R. Delventhal, "The architecture of the electric power system of the international space station and its application as a platform for power technology development," in *Energy Conversion Engineering Conference and Exhibit, 2000. (IECEC) 35th Intersociety*, vol. 2, 2000, pp. 855 –864 vol.2.

[9] R. Cuzner and G. Venkataramanan, "The status of DC micro-grid protection," in *Industry Applications Society Annual Meeting, 2008. IAS '08. IEEE*, Oct. 2008, pp. 1–8.

[10] P. J. Norman, S. J. Galloway, G. M. Burt, D. R. Trainer, and M. Hirst, "Transient analysis of the more-electric engine electrical power distribution network," in *Power Electronics, Machines and Drives, 2008. PEMD 2008. 4th IET Conference on*, April 2008, pp. 681 –685.

[11] J. G. Ciezki and R. W. Ashton, "Selection and stability issues associated with a navy shipboard dc zonal electric distribution system," *Power Delivery, IEEE Transactions on*, vol. 15, no. 2, pp. 665 –669, April 2000.

[12] M. E. Baran and N. R. Mahajan, "Overcurrent protection on voltage-source-converter-based multiterminal dc distribution systems," *Power Delivery, IEEE Transactions on*, vol. 22, no. 1, pp. 406 –412, Jan. 2007.

[13] D. Salomonsson, L. Soder, and A. Sannino, "Protection of low-voltage dc microgrids," *Power Delivery, IEEE Transactions on*, vol. 24, no. 3, pp. 1045 –1053, July 2009.

[14] A. Greenwood and T. Lee, "Generalized damping curves and their use in solving power-switching transients," *Power Apparatus and Systems, IEEE Transactions on*, vol. 82, no. 67, pp. 527 –535, Aug. 1963.

[15] "Short-circuit currents in DC auxiliary installations in power plants and substations Part 1: Calculation of short-circuit currents," IEC 61660-1:1997, 1997.

[16] L. Tang and B.-T. Ooi, "Locating and isolating DC faults in multi-terminal DC systems," *Power Delivery, IEEE Transactions on*, vol. 22, no. 3, pp. 1877 –1884, July 2007.

[17] J. Yang, J. Fletcher, and J. O'Reilly, "Multiterminal dc wind farm collection grid internal fault analysis and protection design," *Power Delivery, IEEE Transactions on*, vol. 25, no. 4, pp. 2308 –2318, oct. 2010.

[18] P. Karlsson and J. Svensson, "Fault detection and clearance in DC distributed systems," in *Nordic Worskshop on Power and Industrial Electronics*, August 2002.

[19] Q. Zhou, M. Sumner, and D. Thomas, "Fault detection for the aircraft distribution systems using impedance estimation," in *Power Electronics, Machines and Drives, 2008. 4th IET Conference on*, 2-4 2008, pp. 666 –670.

[20] L. Han, J. Wang, and D. Howe, "Stability assessment of distributed dc power systems for more-electric aircraft," in *Power Electronics, Machines and Drives, 2008. 4th IET Conference on*, 2-4 2008, pp. 661 –665.

[21] N. Schofield and S. Long, "Generator operation of a switched reluctance starter/generator at extended speeds," *Vehicular Technology, IEEE Transactions on*, vol. 58, no. 1, pp. 48 –56, Jan. 2009.

[22] Z. Xu, B. Zhang, S. Sirisukprasert, X. Zhou, and A. Huang, "The emitter turn-off thyristor-based DC circuit breaker," in *Power Engineering Society Winter Meeting, 2002. IEEE*, vol. 1, 2002, pp. 288 – 293.

[23] "Short-circuit currents in DC auxiliary installations in power plants and substations Part 2: Calculation of effects," IEC 61660-2:1997, 1997.

[24] A. Greenwood, *Electrical Transients in Power Systems*, 2nd ed. Wiley-Interscience, 1991, ch. 3, ISBN: 0-471-62058-0.

[25] P. Sutherland, "DC short-circuit analysis for systems with static sources," *Industry Applications, IEEE Transactions on*, vol. 35, no. 1, pp. 144 –151, Jan/Feb 1999.

[26] "IEEE guide for the protection of stationary battery systems," IEEE Std 1375-1998, 1998.

[27] L. Andrade and C. Tenning, "Design of the Boeing 777 electric system," in *IEEE NAECON 1992*, vol. 3, May 1992, pp. 1281–1290, ISBN: 0-7803-0652-X.

[28] J. C. Cunningham and W. M. Davidson, "A-C and D-C short-circuit tests on aircraft cable," *American Institute of Electrical Engineers, Transactions of the*, vol. 63, no. 12, pp. 961 –969, dec. 1944.

[29] "Interface standard for aircraft/store electrical interconnection system," MIL-STD-1760D, 2003.

[30] Air Accidents Investigation Branch (AAIB) Field Investigation, "Airbus A319-131, G-EUPZ serious incident report," in *AAIB Bulletin*, August 2010.

[31] "Semikron freewheeling diode chip SKCD 81 C 060 I HD [Online]," Available at: http://www.semikron.com/, Datasheet, [Accessed: 12.07.10].

[32] S. Fletcher, P. J. Norman, S. J. Galloway, and G. M. Burt, "Evaluation of overvoltage protection requirements for a DC UAV electrical network," in *SAE Power Systems Conference*, November 2008, paper no. 2008-01-2900.

[33] S. D. A. Fletcher, P. J. Norman, S. J. Galloway, and G. M. Burt, "Mitigation against overvoltages on a DC marine electrical system," in *Electric Ship Technologies Symposium, 2009. ESTS 2009. IEEE*, April 2009, pp. 420 –427.

[34] W. Lu and B.-T. Ooi, "DC overvoltage control during loss of converter in multiterminal voltage-source converter-based HVDC (M-VSC-HVDC)," *Power Delivery, IEEE Transactions on*, vol. 18, no. 3, pp. 915 – 920, July 2003.

[35] S. Krstic, E. L. Wellner, A. R. Bendre, and B. Semenov, "Circuit breaker technologies for advanced ship power systems," in *Electric Ship Technologies Symposium, 2007. ESTS '07. IEEE*, May 2007, pp. 201 –208.

[36] J.-M. Meyer and A. Rufer, "A DC hybrid circuit breaker with ultra-fast contact opening and integrated gate-commutated thyristors (IGCTs)," *Power Delivery, IEEE Transactions on*, vol. 21, no. 2, pp. 646 – 651, April 2006.

[37] M. Steurer, K. Frohlich, W. Holaus, and K. Kaltenegger, "A novel hybrid current-limiting circuit breaker for medium voltage: principle and test results," *Power Delivery, IEEE Transactions on*, vol. 18, no. 2, pp. 460 – 467, April 2003.

[38] "Secheron high-speed DC circuit-breaker for rolling stock type UR26. [Online]," Available at: http://www.secheron.com, Datasheet, [Accessed: 12.07.10].

[39] "Tyco Electronics Aerospace 270VDC Circuit Breaker. [Online]," Available at: http://relays.tycoelectronics.com, Datasheet, [Accessed: 12.07.10].

[40] R. Schmerda, S. Krstic, E. Wellner, and A. Bendre, "IGCTs vs. IGBTs for circuit breakers in advanced ship electrical systems," in *Electric Ship Technologies Symposium, 2009. ESTS 2009. IEEE*, April 2009, pp. 400 –405.

[41] "Network protection and automation guide, chapter 9 overcurrent protection for phase and earth faults. [online]," Available at: http://www.alstom.com/grid, [Accessed: 2.06.11].

[42] A. Siu, "Discrimination of miniature circuit breakers in a telecommunication dc power system," in *Telecommunications Energy Conference, 1997. INTELEC 97., 19th International*, 19-23 1997, pp. 448 –453.

[43] "Network protection and automation guide, chapter 10 unit protection of feeders. [online]," Available at: http://www.alstom.com/grid, [Accessed: 2.06.11].

[44] C. Booth, I. Elders, A. Mackay, J. Schuddebeurs, and J. McDonald, "Power system protection of all electric marine systems," in *Developments in Power System Protection, 2008. DPSP 2008. IET 9th International Conference on*, March 2008, pp. 702 –707.

[45] A. Apostolov, "IEC 61850 based bus protection – principles and benefits," in *Power Energy Society General Meeting, 2009. PES '09. IEEE*, July 2009, pp. 1 –6.

[46] H. Takeda, H. Ayakawa, M. Tsumenaga, and M. Sanpei, "New protection method for HVDC lines including cables," *Power Delivery, IEEE Transactions on*, vol. 10, no. 4, pp. 2035 –2039, Oct 1995.

[47] "Freescale Semiconductor MCF52235 ColdFire integrated microcontroller reference manual [Online]," Available at: http://www.freescale.com/, [Accessed: 12.07.10].

[48] "Infineon TC1796 microcontroller user's manual [Online]," Available at: http://www.infineon.com/, [Accessed: 12.07.10].